

University of Groningen

Pharmacodynamic mechanism-based interaction model for the haemodynamic effects of remifentanil and propofol in healthy volunteers

Su, Hong; Koomen, Jeroen V; Eleveld, Douglas J; Struys, Michel M R F; Colin, Pieter J

Published in:
British Journal of Anaesthesia

DOI:
[10.1016/j.bja.2023.04.043](https://doi.org/10.1016/j.bja.2023.04.043)

IMPORTANT NOTE: You are advised to consult the publisher's version (publisher's PDF) if you wish to cite from it. Please check the document version below.

Document Version
Publisher's PDF, also known as Version of record

Publication date:
2023

[Link to publication in University of Groningen/UMCG research database](#)

Citation for published version (APA):

Su, H., Koomen, J. V., Eleveld, D. J., Struys, M. M. R. F., & Colin, P. J. (2023). Pharmacodynamic mechanism-based interaction model for the haemodynamic effects of remifentanil and propofol in healthy volunteers. *British Journal of Anaesthesia*, 131(2), 222-233. <https://doi.org/10.1016/j.bja.2023.04.043>

Copyright

Other than for strictly personal use, it is not permitted to download or to forward/distribute the text or part of it without the consent of the author(s) and/or copyright holder(s), unless the work is under an open content license (like Creative Commons).

The publication may also be distributed here under the terms of Article 25fa of the Dutch Copyright Act, indicated by the "Taverne" license. More information can be found on the University of Groningen website: <https://www.rug.nl/library/open-access/self-archiving-pure/taverne-amendment>.




Take-down policy

If you believe that this document breaches copyright please contact us providing details, and we will remove access to the work immediately and investigate your claim.

Downloaded from the University of Groningen/UMCG research database (Pure): <http://www.rug.nl/research/portal>. For technical reasons the number of authors shown on this cover page is limited to 10 maximum.

CARDIOVASCULAR

Pharmacodynamic mechanism-based interaction model for the haemodynamic effects of remifentanyl and propofol in healthy volunteers

Hong Su¹, Jeroen V. Koomen^{1,2}, Douglas J. Eleveld¹, Michel M. R. F. Struys^{1,3} and Pieter J. Colin^{1,*}

¹Department of Anesthesiology, University Medical Center Groningen, University of Groningen, Groningen, the Netherlands, ²Department of Pharmacology, Toxicology and Kinetics, Dutch Medicines Evaluation Board, Utrecht, the Netherlands and ³Department of Basic and Applied Medical Sciences, Ghent University, Ghent, Belgium

*Corresponding author. E-mail: p.j.colin@umcg.nl

Preliminary results presented at the 2021 Pharmacokinetics UK meeting, November 11, 2022; 2021 American Society of Anesthesiologists Annual Meeting, October 8–12, 2022; and 2022 Quantitative Systems Pharmacology Conference, Leiden, the Netherlands, April 20–22, 2022.

Abstract

Background: Propofol and remifentanyl are frequently combined for the induction and maintenance of general anaesthesia. Both propofol and remifentanyl cause vasodilation and potentially reduce arterial BP. We aimed to develop a mechanism-based model that characterises the haemodynamic interactions between remifentanyl and propofol.

Methods: Data from two clinical trials in healthy volunteers were analysed using remifentanyl-alone, propofol-alone, and combination groups. We evaluated remifentanyl effects on haemodynamics using a previously developed mechanism-based haemodynamic model of propofol. The interaction between propofol and remifentanyl was explored using the principles of the general pharmacodynamic interaction (GPDI) model.

Results: Remifentanyl alone increased the dissipation rate of total peripheral resistance by 50% at 3.0 ng ml⁻¹. Additionally, the dissipation rates of HR and stroke volume were attenuated by 4.8% and 4.9% per 1 ng ml⁻¹ increase in remifentanyl concentration, respectively. The maximal effect of propofol alone in decreasing the production rate of total peripheral resistance was 78%, which decreased to 32% when combined with remifentanyl 4 ng ml⁻¹. The effects of remifentanyl on HR and stroke volume were attenuated by propofol with maximum decreases of 11.9% and 21.2%, respectively. Goodness-of-fit plots and prediction-corrected visual predictive check plots showed good predictive performance of the models.

Conclusions: The structure of the previous mechanism-based haemodynamic model for propofol was able to describe the effects of remifentanyl alone on haemodynamic variables. The GPDI model provided a good framework for characterising the pharmacodynamic interaction between remifentanyl and propofol on haemodynamic properties.

Clinical trial registration: NCT02043938; NCT03143972.

Keywords: haemodynamic; healthy volunteers; interaction; mechanism-based pharmacodynamic modelling; propofol; remifentanyl

Received: 11 January 2023; Accepted: 27 April 2023

© 2023 The Author(s). Published by Elsevier Ltd on behalf of British Journal of Anaesthesia. This is an open access article under the CC BY license (<http://creativecommons.org/licenses/by/4.0/>).

For Permissions, please email: permissions@elsevier.com

Editor's key points

- Remifentanyl and propofol are frequently combined during general anaesthesia in clinical practice, but few empirical models have investigated the interactions between remifentanyl and propofol on cardiovascular function.
- A general pharmacodynamic interaction model identified an antagonistic interaction on heart rate, a synergistic interaction on stroke volume, and a mixed synergistic–antagonistic interaction on mean arterial pressure between remifentanyl and propofol.
- This study extends a previously described mechanism-based haemodynamic model for propofol to quantify the haemodynamic effects of remifentanyl and their interactions to facilitate prediction of the haemodynamic effects of general anaesthesia.

Remifentanyl is a short-acting μ -opioid agonist with analgesic properties,¹ and propofol is an allosteric agonist of the Type A γ -aminobutyric acid receptor that is a fast-acting hypnotic drug.² The combination of these drugs is frequently used for induction and maintenance of sedation and general anaesthesia in clinical practice. However, both remifentanyl and propofol have dose-dependent haemodynamic side-effects.^{2–4} Hypotension induced by general anaesthesia is associated with increased postoperative morbidity and mortality.⁵ Understanding the relationship between exposure to anaesthetic drugs and haemodynamic variables could contribute to preventing haemodynamic side-effects, such as hypotension, in clinical practice.

The haemodynamic side-effects of remifentanyl are caused by vagal activation, which results in reduced MAP, cardiac output, and systemic vascular resistance.^{1,3} The haemodynamic side-effects of propofol are the results of a decrease in sympathetic tone, which reduces total peripheral resistance (TPR) and thereby lowers MAP.² Propofol also lowers stroke volume (SV) by decreasing the preload of the left ventricle.^{6,7}

The haemodynamic effects of propofol have been described previously in a mechanism-based haemodynamic model in healthy volunteers.⁷ The haemodynamic effects of remifentanyl on MAP have only been described empirically without consideration of feedback mechanisms between TPR, SV, HR, and MAP.⁸ The interaction between remifentanyl and propofol on MAP and HR separately has been quantified using response surface models.⁹ However, response surface models have limitations because they draw inference on the types of interactions between two drugs (infra-additive, additive, or synergistic) at the effect level only, by comparing a predicted additive response based on the single-drug effect using an additivity model (e.g. Loewe additivity or Bliss independence) with the observed response. Although useful for qualifying drug interactions, response surface models are less useful for simulation, as they do not quantify the interaction at the parameter level. In contrast, mechanism-based models with drug effects incorporated using the general pharmacodynamic interaction (GPDI) model do not have these limitations. The two primary aims of this study were therefore (i) to extend the previously developed mechanism-based haemodynamic model of propofol to characterise the effect of remifentanyl alone on haemodynamic variables in healthy volunteers, and

(ii) to describe the interaction between remifentanyl and propofol on haemodynamic variables quantitatively using the GPDI model.

Methods**Study design**

Data from two clinical trials^{10,11} in healthy volunteers without surgical stimuli were re-analysed in this study. Data for the remifentanyl-alone group were obtained from the trial by Weerink and colleagues,¹⁰ which was approved by the Foundation for the Evaluation of Ethics in Biomedical Research, Assen, the Netherlands (Medical Research Ethics Committee approval number NL61190.056.17) and registered at [ClinicalTrials.gov](https://clinicaltrials.gov) (NCT03143972). A total of 30 volunteers received a target-controlled infusion (TCI) of remifentanyl in a step-up manner at effect-site target concentrations of 1, 2, 3, 5, and 7 ng ml⁻¹ using the Eleveld pharmacokinetic model,¹² followed by a 30 min washout. Each target was maintained for 12 min to reach equilibrium, and blood samples were taken at the end of the equilibration time.¹⁰ The trial by Kuizenga and colleagues¹¹ was approved by the Institutional Review Board of the University Medical Center Groningen (NL43238.042.13) and registered at [ClinicalTrials.gov](https://clinicaltrials.gov) (NCT02043938), and it included healthy volunteers stratified by age and sex. Volunteers received drug infusions on two separate days. On the first day, each volunteer received propofol using TCI in a step-up and step-down titration scheme targeting effect-site concentrations of 0.5, 1, 1.5, 2.5, 3.5, 4.5, 6, and 7.5 μ g ml⁻¹ followed by a single bolus using the Schnider pharmacokinetic–pharmacodynamic model (the propofol-alone group).^{13,14} On the second day (>1 week after the first study day), volunteers were randomised across two (2 or 4 ng ml⁻¹) remifentanyl groups, and they were again dosed according to the same step-up and step-down scheme for propofol. Remifentanyl was administered via TCI using the Minto pharmacokinetic–pharmacodynamic model (the combination group).^{15,16}

Haemodynamic measurements and data handling

In the trial by Weerink and colleagues,¹⁰ systolic BP, diastolic BP, and MAP were measured using a radial artery catheter (IntelliVue MP70® monitor; Philips, Amsterdam, the Netherlands). HR was derived from standard three-lead ECG. All variables were collected every 15 s using RugloopII software (Demed, Temse, Belgium). In the trial by Kuizenga and colleagues,¹¹ ECG and noninvasive BP measurements were obtained from a Philips IntelliVue MP50 vital signs monitor (Philips Medizin Systeme, Böblingen, Germany). Noninvasive MAP, systolic BP, and diastolic BP were measured every minute. HR was derived from the ECG and was recorded every second. All variables were collected using RugloopII software. Pulse pressure (PP) was calculated from the measured systolic and diastolic BP in both studies.

For the remifentanyl-alone group, invasive haemodynamic measurements were influenced by the collection of blood samples. To account for this influence, we removed HR and BP measurements 2 min before and after the time of blood sample collection. We applied a median filter to reduce the influence of artifacts in the data or outlying observations for the remifentanyl-alone and combination groups, as described.⁷

Population pharmacokinetic–pharmacodynamic modelling

Pharmacokinetics of remifentanil and propofol

The pharmacokinetics of remifentanil and propofol were characterised using the individual pharmacokinetic parameter approach.¹⁷ Individual *post hoc* pharmacokinetic parameters (CL, Q2, Q3, V1, V2, and V3) for remifentanil and propofol were derived from the Eleveld pharmacokinetic models for remifentanil¹² and propofol.¹⁸

Mechanism-based haemodynamic model of remifentanil

Data from the remifentanil-alone group were used to develop a mechanism-based haemodynamic model for remifentanil. The structural model was based on the previously described mechanism-based haemodynamic model for propofol.⁷ In the structural model, PP was used as a surrogate of SV (SV/PP=1.5).⁷ Remifentanil drug effects were explored on turnover equations of TPR, SV, and HR using linear, log-linear, E_{\max} , and sigmoid E_{\max} models. The remifentanil drug effects were implemented on zero-order production rate constants (k_{in}) or first-order dissipation rate constants (k_{out}) of the turnover equations. Time-dependent effects were further explored to describe elevated MAP, HR, and PP before the start of the remifentanil infusion. Correlations between covariates and *post hoc* predicted parameters, for which between-subject variability (BSV) was included, were graphically explored. The potential influence of covariate effects was formally evaluated by comparing the change in objective function value (OFV) between competing models. The criteria for inclusion of covariates were a decrease in OFV of >3.84 points. Age, weight, height, sex, and BMI were considered as potential covariates.

Mechanism-based haemodynamic model for combined remifentanil and propofol infusions

On top of the time-dependent effects on HR, we explored time-dependent effects on TPR and SV for the mechanism-based haemodynamic model for propofol. The mechanism-based haemodynamic model for the combination of remifentanil and propofol (further referred to as the interaction model) was investigated using the GPDI model.¹⁹ Data from the remifentanil-alone, propofol-alone, and combination groups were simultaneously fitted to develop the interaction model.

In the GPDI model, the effects of remifentanil (E_{\max} or linear model) on haemodynamics can be altered concentration-dependently by propofol and vice versa. Example model structures are displayed in the box, where remifentanil and propofol can interact with each other on E_{\max} [equations (1) and (2)] or EC_{50} [equations (3) and (4)] if the drug effect is implemented by the E_{\max} model, or on the slope for linear effect [equation (5)] **Box 1**.

In these equations, E_{PROP} and E_{REMI} represent the effects of propofol and remifentanil, respectively; E_{\max_PROP} and E_{\max_REMI} are the maximum effects of propofol and remifentanil, respectively; EC_{50_PROP} and EC_{50_REMI} represent the propofol and remifentanil concentrations that produce 50% of the maximum drug effects, respectively; C_{P_PROP} and C_{P_REMI} represent the plasma concentrations of propofol and remifentanil, respectively; γ_{PROP} and γ_{REMI} represent the Hill coefficients for propofol and remifentanil, respectively; SL_{REMI} is the slope of the linear effects of remifentanil; and INT_{PR}

Box 1

Equations for an example GPDI model.

$$E_{PROP} = \frac{E_{\max_PROP} \times \left(1 + \frac{INT_{PR} \times C_{P_REMI}}{EC_{50_INT_PR} + C_{P_REMI}}\right) \times C_{P_PROP}^{\gamma_{PROP}}}{EC_{50_PROP}^{\gamma_{PROP}} + C_{P_PROP}^{\gamma_{PROP}}} \quad (1)$$

$$E_{REMI} = \frac{E_{\max_REMI} \times \left(1 + \frac{INT_{PR} \times C_{P_PROP}}{EC_{50_INT_PR} + C_{P_PROP}}\right) \times C_{P_REMI}^{\gamma_{REMI}}}{EC_{50_REMI}^{\gamma_{REMI}} + C_{P_REMI}^{\gamma_{REMI}}} \quad (2)$$

$$E_{PROP} = \frac{E_{\max_PROP} \times C_{P_PROP}^{\gamma_{PROP}}}{EC_{50_PROP}^{\gamma_{PROP}} \times \left(1 + \frac{INT_{PR} \times C_{P_REMI}}{EC_{50_INT_PR} + C_{P_REMI}}\right) + C_{P_PROP}^{\gamma_{PROP}}} \quad (3)$$

$$E_{REMI} = \frac{E_{\max_REMI} \times C_{P_REMI}^{\gamma_{REMI}}}{EC_{50_REMI}^{\gamma_{REMI}} \times \left(1 + \frac{INT_{PR} \times C_{P_PROP}}{EC_{50_INT_PR} + C_{P_PROP}}\right) + C_{P_REMI}^{\gamma_{REMI}}} \quad (4)$$

$$EFF_{REMI} = \left(SL_{REMI} + \frac{INT_{PR} \times C_{P_PROP}}{EC_{50_PROP} + C_{P_PROP}}\right) \times C_{P_REMI} \quad (5)$$

represents the magnitude of the maximum change in E_{\max} of propofol caused by remifentanil and vice versa for INT_{PR} .

When the interaction terms are implemented for E_{\max} (equations 1 and 2), interpretations of the INT parameters are as follows: $INT_{PR}=0$ indicates no interaction; $INT_{PR} >0$ indicates an increase in E_{\max} , representing synergy; and $INT_{PR} <0$ indicates a decrease in E_{\max} , representing antagonism. When the interaction terms are implemented for EC_{50} [equations (3) and (4)], interpretation of the INT parameters are as follows: $INT_{PR}=0$ indicates no interaction; $INT_{PR} >0$ indicates an increase in EC_{50} , representing antagonism; and $-1 < INT_{PR} < 0$ indicates a decrease in C_{50} , representing synergy.

As a starting point for development of the interaction model, we considered a model without interactions (the combination-null interaction model, $INT=0$). Refinements to this model, in line with the structure of the GPDI model, were explored in a sequential approach (i.e. adding one interaction term at a time). The criteria for inclusion of an interaction effect in the model were a decrease in OFV of >3.84 points, improvement in the prediction-corrected visual predictive checks, and standard goodness-of-fit plots. We also applied backward elimination on the final model and excluded interaction terms if OFV increased <6.64 points (the 1% significance level critical quantile of the corresponding χ^2 distribution) upon removal of a specific interaction component.

Parameter estimation and model evaluation

Data were fitted using the first-order conditional estimation method with interaction using NONMEM (version 7.5; Icon Development Solutions, Hannover, MD, USA). ADVAN13 and tolerance 12 subroutines were applied in the estimation. BSV was described using exponential or additive models. Residual variability was estimated using additive or proportional error models. Goodness of fit was graphically evaluated by plotting the individual or population predictions vs the observations and the conditionally weighted residuals vs population predictions and time. Parameter uncertainty of the models was estimated using the covariance step in NONMEM or sampling importance resampling.²⁰ Prediction-corrected visual predictive checks were used to evaluate models internally.²¹ All models and simulations were run using PsN (version 5.2.6)²² and Pirana (version 3.0.0)²³ as back end and front end to NONMEM. Graphical assessment of goodness of fit and

simulations and construction of prediction-corrected visual predictive checks were conducted in R (R Foundation for Statistical Computing, Vienna, Austria).²⁴

Simulations of the interaction model

The final interaction model was used to simulate the concentration–effect relationship for MAP, HR, and SV for a 35-yr-old individual receiving propofol or propofol plus remifentanyl 2 or 4 ng ml⁻¹. Similar simulations were produced for the combination-null interaction model to evaluate the clinical relevance of the differences in predictions between the combination-null interaction model (INT=0) and the final interaction model.

Finally, we performed 1000 simulations to predict the expected changes in haemodynamics when remifentanyl and propofol are administered simultaneously according to the dosing recommendations described in the propofol²⁵ and remifentanyl²⁶ US Food and Drug Administration (FDA)-approved drug labelling. According to the label, adults (<55 yr of age) should receive propofol at an induction dose of 1.5 mg kg⁻¹ over 60 s, followed by a maintenance dose of 0.1 mg kg⁻¹ min⁻¹, along with a continuous infusion of remifentanyl at 0.1 µg kg⁻¹ min⁻¹. We simulated the haemodynamic effects for three people (aged 22, 47, and 60 yr), which represent the median age of the three age groups in the pooled study dataset. These typical individuals were assumed to be males weighing 70 kg with a height of 180 cm.

Results

The patient characteristics of the healthy volunteers are summarised in [Supplementary Tables 2–1](#). In summary, 30 and 36 individuals stratified by age and sex were included in the remifentanyl-alone and propofol-alone groups. Individuals in the propofol-alone group were then randomly separated into two combination groups (propofol combined with remifentanyl 2 or 4 ng ml⁻¹). The measured plasma concentrations of remifentanyl and propofol and the observed MAP, HR, and PP for both the remifentanyl-alone and combination groups are shown in [Supplementary Figs. 2–1, 2-2, and 2-3](#).

No bias for either the Eleveld remifentanyl and Eleveld propofol pharmacokinetic models ([Supplementary Figs. 1–1, 1-2, and 1-3](#)) was observed in the pharmacokinetic prediction for simultaneous administration of both drugs.

For the remifentanyl-alone group, the median MAP decreased from 90 mm Hg [95% quantile: 72–112 mm Hg] at baseline to 77 mm Hg [95% quantile: 57–96 mm Hg] at the target concentration of 2 ng ml⁻¹, and then it increased to 82 mm Hg [95% quantile: 64–102 mm Hg] at the target concentration of 7 ng ml⁻¹. Similarly, PP decreased from 74 mm Hg [95% quantile: 45–93 mm Hg] to 61 mm Hg [95% quantile: 36–78 mm Hg] at 2 ng ml⁻¹, and then it increased to 64 mm Hg [95% quantile: 38–110 mm Hg] at the target concentration of 7 ng ml⁻¹. HR decreased from 60 beats min⁻¹ [95% quantile: 48–85 beats min⁻¹] at baseline to 57 beats min⁻¹ [95% quantile: 46–75 beats min⁻¹] at the target concentration of 2 ng ml⁻¹, and it increased to 66 beats min⁻¹ [95% quantile: 44–100 beats min⁻¹] at the target concentration of 7 ng ml⁻¹.

For the combination group, the median MAPs were 55 mm Hg [95% quantile: 52–81 mm Hg] and 51 mm Hg [95% quantile: 43–59 mm Hg] when propofol was combined with remifentanyl 2 and 4 ng ml⁻¹, respectively, at a propofol target concentration of 7.5 µg ml⁻¹. When combined with remifentanyl 2 ng

ml⁻¹, the median HR changed slightly (varied within 59–67 beats min⁻¹), and when combined with remifentanyl 4 ng ml⁻¹, it remained stable (varied within 62–69 beats min⁻¹) at low propofol concentrations and increased at a propofol target concentration of 7.5 µg ml⁻¹ (median HR: 84 beats min⁻¹ [95% quantile: 68–108 beats min⁻¹]). Changes in MAP, HR, and PP for propofol alone and the combination at different propofol target concentrations are summarised in [Table 1](#).

Development of the interaction model

Development of the mechanism-based haemodynamic model of remifentanyl is described in [Supplementary material 3](#). In brief, the structure of the mechanism-based haemodynamic model for remifentanyl is the same as the previously described mechanism-based model for propofol.⁷ Remifentanyl effects were implemented on k_{out} for TPR (sigmoid E_{max} model), HR (linear model), and SV (linear model). Time-dependent effects were addressed on HR and SV. We also explored an additional time-dependent effect on SV in our mechanism-based haemodynamic model of propofol,⁷ and OFV decreased by –271.1.

For development of the interaction model, the mechanism-based model was defined as the combination-null interaction model, and the deviation from this mechanism-based model prediction from the single-drug data was characterised by the GPDI model. Inclusion of an interaction term (propofol influences remifentanyl) for the effect of remifentanyl on HR significantly improved model fit ($\Delta OFV = -224.5$) compared with the combination-null interaction model. The model was further expanded by inclusion of interaction terms for drug effects on TPR (propofol influences remifentanyl, $\Delta OFV = -297.7$, and remifentanyl influences propofol, $\Delta OFV = -175.7$). Finally, an interaction term for the effect of remifentanyl on SV (propofol influences remifentanyl, $\Delta OFV = -1132.2$) was included. During backward elimination, OFV decreased by 23.3 points when excluding the interaction term for TPR (propofol affecting remifentanyl), so this effect was removed from the model. We further modified the model by fixing the Hill coefficient of remifentanyl on the effect on TPR to 1 because of instability in the parameter estimation, despite an OFV increase by 60.6 points. Prediction-corrected visual predictive checks and goodness-of-fit plots were not different after fixing these model parameters.

Final interaction model

The final interaction model is shown in equations (6)–(17) ([Boxes 2 and 3](#)), with the structure of the model shown in [Fig. 1](#) and the code of the final interaction model presented in [Supplementary material 6](#). Parameter estimates and associated relative standard errors for the interaction model are shown in [Table 2](#).

The variables k_{in_TPR} , k_{in_SV} , and k_{in_HR} represent the zero-order production rate constants, and k_{out} is the first-order dissipation rate constant of TPR, SV, and HR. SV^* represents the SV affected by the negative change in MAP and drug effect. HR^* represents the HR influenced by the feedback of MAP. RMAP is MAP normalised to baseline values. FB is the power term of the negative feedback of MAP on TPR, SV, and HR. HR_SV is a constant that represents the magnitude of the direct inverse effect of HR on SV. $E_{max_PROP_TPR}$, $E_{max_PROP_SV}$, and $E_{max_REML_TPR}$ are the maximal effects of propofol on TPR, SV, and remifentanyl on TPR, respectively. EC_{50PROP_TPR} ,

Table 1 Observed median and 95% quantile for MAP, HR, and pulse pressure (PP) at different propofol effect-site target concentrations for propofol alone and combined with two remifentanyl effect-site concentrations.

Propofol target concentration ($\mu\text{g ml}^{-1}$)	Variable	0	0.5	1	1.5	2.5	3.5	4.5	6	7.5
Propofol alone	MAP (mm Hg)	81 [59–108]	86 [65–104]	80 [64–100]	73 [57–99]	70 [53–100]	65 [49–95]	63 [47–91]	57 [45–80]	55 [44–75]
	HR (beats min^{-1})	63 [41–83]	61 [37–77]	62 [41–81]	65 [42–87]	67 [49–93]	72 [54–102]	74 [55–105]	76 [55–104]	86 [67–105]
	PP (mm Hg)	50 [29–78]	44 [24–70]	47 [27–69]	47 [27–70]	50 [28–73]	51 [28–73]	53 [28–73]	58 [29–73]	61 [44–76]
Propofol plus remifentanyl 2 ng ml^{-1}	MAP (mm Hg)	79 [55–113]	76 [57–98]	68 [54–100]	65 [49–98]	58 [45–94]	55 [44–84]	56 [47–73]	57 [49–80]	55 [52–81]
	HR (beats min^{-1})	65 [46–86]	59 [43–80]	59 [44–72]	59 [46–89]	62 [48–81]	63 [57–80]	65 [58–74]	67 [60–73]	67 [63–72]
	PP (mm Hg)	51 [30–81]	53 [32–82]	50 [31–77]	49 [31–73]	49 [31–70]	48 [31–68]	49 [28–71]	50 [39–75]	52 [42–73]
Propofol plus remifentanyl 4 ng ml^{-1}	MAP (mm Hg)	81 [51–113]	81 [59–116]	69 [51–114]	62 [45–100]	59 [43–82]	60 [41–77]	62 [43–78]	57 [43–79]	51 [43–59]
	HR (beats min^{-1})	69 [45–103]	62 [42–95]	63 [42–95]	62 [42–88]	62 [45–88]	65 [49–91]	67 [51–101]	80 [52–108]	84 [68–108]
	PP (mm Hg)	52 [33–84]	52 [30–85]	49 [30–79]	48 [28–77]	50 [24–74]	50 [26–71]	51 [32–70]	54 [38–72]	55 [40–69]

EC_{50PROP_SV} , and EC_{50REMI_TPR} are the concentrations that produce 50% of the maximal effect of propofol on TPR, SV, and remifentanyl on TPR, respectively. INT_{TPR} is the maximum magnitude change of E_{max} of propofol on TPR caused by remifentanyl. SL_{REMI_SV} and SL_{REMI_HR} are the slopes of the linear effects of remifentanyl on SV and HR, respectively. INT_{SV} and INT_{HR} represent the maximum magnitude changes of slope of remifentanyl on SV and HR caused by propofol, respectively. EC_{50INT_HR} is the interaction potency of propofol on the effect of remifentanyl on HR.

The effects of remifentanyl and propofol on TPR, HR, and SV and the interaction between remifentanyl and propofol are shown in equations (12)–(16) (Box 3). In line with the mechanism-based haemodynamic model for propofol,⁷ the effect of age on the E_{max} of SV of propofol was confirmed in the interaction model ($\Delta OFV = -1737$), indicating $E_{max_PROP_SV}$ increases with increasing age [equation (17)].⁷ In equation (17), $E_{max_PROP_SV}$ (typ) is the population typical value of the maximal effect of propofol on SV:

The final estimations of baseline MAP, HR, and SV were 75 mm Hg, 56 beats min^{-1} , and 83 ml, respectively. The apparent MAP [taking into account the time-dependent effect described in equations (8) and (9)] was 92 mm Hg, which resulted from an increase in HR by 7 beats min^{-1} and an increase in SV by 7.4 ml before drug administration. The estimated drug effect parameters for the interaction model are comparable with the single models (mechanism-based haemodynamic model for remifentanyl and propofol). For instance, the estimated E_{max} for the reduced production rate of TPR (77.8% for the interaction model vs 86.0% for the propofol model) of propofol are similar in the single models and interaction model.

According to our final model, HR and SV increased by 3.3% and 5.8% from baseline per 1 ng ml^{-1} increase in remifentanyl concentration (remifentanyl alone). The positive effect of remifentanyl on HR and SV was attenuated by propofol. (INT_{HR} and INT_{SV} are negative.) This negative interaction was also reflected in Figs. 2 and 3, for remifentanyl combined with propofol, when the elevated HR was reduced (purple line vs blue line). For SV, the increased SV was reversed when propofol was combined with remifentanyl. For TPR, the maximal effect of propofol in decreasing the production rate of TPR was 77.8% when combined with remifentanyl 2 or 4 ng ml^{-1} , and the maximal effects of propofol on TPR were reduced to 47.5% and 31.2% (calculated from $E_{max_PROP_TPR}$ and INT_{TPR} , respectively).

The goodness-of-fit plots (Supplementary Figs 4–1 to 4–12) and prediction-corrected visual predictive check plots (Supplementary Figs 4–13 to 4–24) showed the model could adequately describe our data with good predictive performance. The diagnostic plots of sampling importance resampling are shown in Supplementary Fig. 4–25.

Effects of remifentanyl and propofol combined on haemodynamics

Figs. 2 and 3 show the steady-state plasma concentration–effect relationship (change from baseline) of MAP (left), HR (middle), and SV (right) in a 35-yr-old individual for propofol alone predicted by the mechanism-based haemodynamic model for propofol (purple), propofol combined with remifentanyl 2 or 4 ng ml^{-1} predicted by the combination-null interaction model (green), and the combination interaction

Box 2

Equations of the final interaction model.

$$\frac{dTPR}{dt} = k_{in_TPR} \cdot RMAP^{FB} \cdot (1 + EFF_{PROP_TPR}) - k_{out} \cdot TPR \cdot (1 - EFF_{REMI_TPR}) \quad (6)$$

$$\frac{dSV^*}{dt} = k_{in_SV} \cdot RMAP^{FB} \cdot (1 + EFF_{PROP_SV}) - k_{out} \cdot SV^* \cdot (1 - EFF_{REMI_SV}) \quad (7)$$

$$\frac{dHR^*}{dt} = k_{in_HR} \cdot RMAP^{FB} - k_{out} \cdot HR^* \cdot (1 - EFF_{REMI_HR}) \quad (8)$$

$$SV = (SV^* + TDE_{SV}) \cdot \left[1 - HR_{SV} \cdot \ln\left(\frac{HR}{Base_{HR}}\right) \right] \quad (9)$$

$$HR = HR^* + TDE_{HR} \quad (10)$$

$$RMAP = \frac{HR \cdot SV \cdot TPR}{Base_{HR} \cdot Base_{SV} \cdot Base_{TPR}} \quad (11)$$

Box 3

Equations of the effects of remifentanyl and propofol on total peripheral resistance, heart rate and stroke volume.

$$EFF_{PROP_TPR} = \frac{\left(E_{max_PROP_TPR} + \frac{INT_{TPR} \times C_{P_REMI}}{EC_{50REMI} + C_{P_REMI}} \right) \times C_{P_PROP}^{Y_PROP}}{EC_{50P_PROP}^{Y_PROP} + C_{P_PROP}^{Y_PROP}} \quad (12)$$

$$EFF_{REMI_SV} = \left(SL_{REMI_SV} + \frac{INT_{SV} \times C_{P_PROP}}{EC_{50SV_PROP} + C_{PROP}} \right) \times C_{P_REMI} \quad (13)$$

$$EFF_{REMI_HR} = \left(SL_{REMI_HR} + \frac{INT_{HR} \times C_{P_PROP}}{EC_{50INT_HR} + C_{PROP}} \right) \times C_{P_REMI} \quad (14)$$

$$EFF_{PROP_SV} = \frac{E_{max_PROP_SV} \times C_{P_PROP}}{C_{50PROP_SV} + C_{P_PROP}} \quad (15)$$

$$EFF_{REMI_TPR} = \frac{E_{max_REMI_TPR} \times C_{P_REMI}}{EC_{50REMI_TPR}^{Y_REMI} + C_{P_REMI}} \quad (16)$$

$$E_{max_PROP_SV} = E_{max_PROP_SV(tp)} \cdot e^{(0.033 \cdot (age - 35))} \quad (17)$$

model (blue). When combined with remifentanyl 2 ng ml⁻¹, the effect on MAP of propofol combined with remifentanyl is greater than the effect of propofol alone at low propofol concentrations (<7.5 µg ml⁻¹). When combined with remifentanyl 4 ng ml⁻¹, the effect on MAP for propofol combined with remifentanyl is greater than the effect of propofol alone across the propofol concentration range. The deviation of effect on MAP between propofol alone and propofol combined with remifentanyl was maximal at a propofol concentration of 1.1 µg ml⁻¹, where MAP decreased by 5.7%, 14.6%, and 21.5% for propofol alone and propofol combined with remifentanyl 2 or 4 ng ml⁻¹, respectively. HR increased by 52.3%, 12.3%, and 1.9% from baseline for propofol alone and propofol combined with remifentanyl 2 and 4 ng ml⁻¹, respectively.

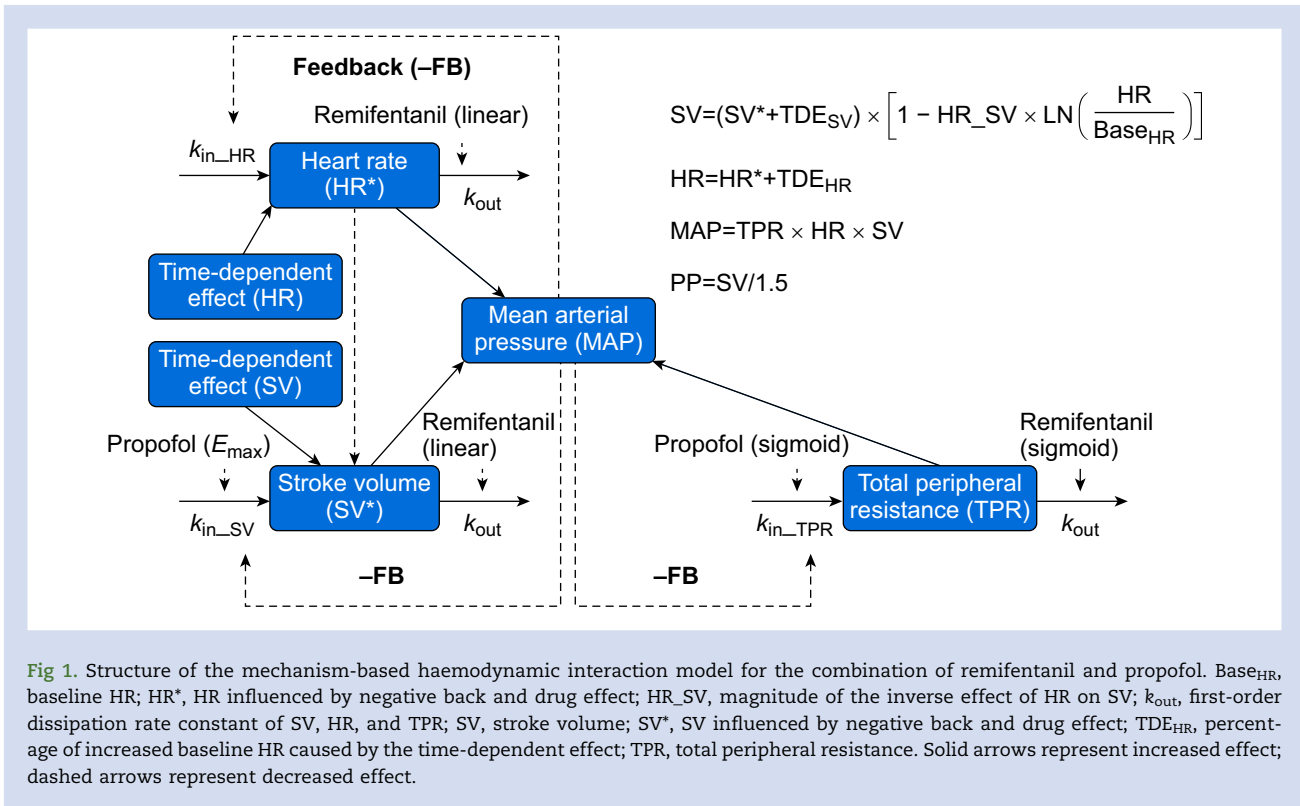
There is an antagonistic interaction between remifentanyl and propofol on HR, which can be seen by comparing blue (combination interaction model) and green (combination-null interaction model) lines. For example, when propofol was combined with remifentanyl 4 ng ml⁻¹, the predicted changes in HR were 12.3% and 24.3% for the interaction model and combination-null interaction model. The predicted decrease in SV for the combination interaction model (32.5%) is stronger than the combination-null interaction model (7.2%) when propofol was combined with remifentanyl 4 ng ml⁻¹, which indicates a synergistic interaction. For MAP, when propofol is combined with remifentanyl 2 ng ml⁻¹ at low propofol concentrations, the effect simulated by the combination interaction model is greater than the combination-null interaction model, whereas at high propofol concentrations, the effect of

the combination interaction model is lower than the combination-null interaction model. There is a synergistic interaction on MAP when propofol is combined with remifentanyl 4 ng ml⁻¹.

Fig. 4 shows the changes in propofol plasma concentration; remifentanyl plasma concentration; and relative changes in MAP, HR, and SV from baseline after propofol combined with remifentanyl according to the FDA drug label for three individuals of different ages.^{25,26} The maximal effect on MAP and SV increased with increasing age (median MAP decreased 32.2% [95% prediction interval: 25.5–37.2%], 36.1% [95% prediction interval: 29.1–41.3%], and 39.6% [95% prediction interval: 32.6–44.9%]) from baseline for individuals aged 22, 47, and 66 yr, whilst median SV decreased to 14.0% [95% prediction interval: 3.2–21.6%], 23.6% [95% prediction interval: 12.6–30.6%], and 32.3% [95% prediction interval: 22.2–38.7%], respectively. Median HR changed slightly (<10% change from baseline) during dosing according to FDA drug label dosing in the three age groups.

Discussion

The structural model of the previously developed mechanism-based haemodynamic model for propofol⁷ was also suitable for quantifying the effects of remifentanyl on haemodynamic variables. Remifentanyl alone decreased TPR and slightly increased HR and PP by altering the dissipation rates of these haemodynamic variables in a concentration-dependent manner. No pharmacokinetic interaction was observed



between propofol and remifentanyl; therefore, quantification of drug–drug interaction focused on haemodynamic variables. The GPDI model was able to describe the drug effects on haemodynamic variables for both single drugs alone and the interaction between remifentanyl and propofol. Three interaction effects between remifentanyl and propofol were identified using the GPDI model that could not be described using the combination-null interaction model. Propofol reduced the effect of remifentanyl on HR and SV, and conversely remifentanyl reduced the propofol effect on TPR. Variability between subjects in all haemodynamic variables was adequately described by the model.

The fundamental framework of our mechanistic model was developed based on a model presented by Snelder and colleagues.²⁷ The pressure–volume loop theory has been used to further update the original model of Snelder and colleagues²⁷ by integrating contractility with cardiac output, as this provided a more mechanistic basis for application of the model.²⁸ We were not able to use this updated model because it is difficult to measure contractility in humans. Nevertheless, performance of the developed mechanism-based model was acceptable in terms of model fit and prediction of haemodynamic variables. We confirm that the structural model of the mechanism-based haemodynamic model for propofol⁷ was also suitable for quantifying the drug effects of remifentanyl on haemodynamic variables.

Remifentanyl is known to produce cardiovascular depression via vagal–cardiac activation, which is thought to originate from peripheral vasodilation leading to hypotension.^{1,3} Some studies have shown that remifentanyl can cause bradycardia, possibly because of a decrease in sympathetic tone and an

increase in vagal tone as a result of stronger intraoperative anti-nociceptive properties.^{3,29,30} Subjects were dosed with both remifentanyl and propofol, and as such, it is not clear whether the observed bradycardia is attributable to remifentanyl or the combination of remifentanyl and propofol. Some studies report tachycardia after dosing with remifentanyl alone, which is in line with our findings, as remifentanyl increased HR. This might be attributable to negative feedback of the baroreflex system caused by hypotension.^{1,31}

Bouillon and colleagues³² have shown that co-administration of propofol and remifentanyl reduces the central volume of distribution and clearance of remifentanyl. Our analysis did not indicate a similar pharmacokinetic interaction between remifentanyl and propofol. We therefore do not expect an influence of combined administration of remifentanyl and propofol on the pharmacokinetics of the individual drugs. Thus, co-administration of remifentanyl and propofol did not influence model performance of the mechanism-based interaction model.

The pharmacodynamic drug–drug interaction between remifentanyl and propofol on haemodynamics has been investigated by Nieuwenhuijs and colleagues.⁹ They developed models for HR and MAP separately using response surface modelling and found additive interactions between remifentanyl and propofol. We applied GPDI model principles to describe the pharmacodynamic drug–drug interaction between remifentanyl and propofol, which allows us to predict both single-drug effects and interactions without changing the single-model structures.¹⁹ Using this approach, a non-additive interaction between propofol and remifentanyl could be quantified, which differs from the model of

Table 2 Parameter estimates of final interaction model. *Calculated according to $\sqrt{e^{\sigma^2} - 1} \times 100\%$. Base_{SV}, Base_{HR}, and Base_{TPR}, baseline SV, HR, and TPR; BSV, between-subject variability; EC_{50TPR}, concentrations that produce half of the maximal remifentanyl effect of TPR; E_{max_TPR}, maximum effect of remifentanyl on TPR; FB, magnitude of the feedback; FIX, parameter values kept unchanged during estimation; HR_{SV}, magnitude of the inverse effect of HR on SV; k, first-order dissipation rate constant of the time-dependent effect; k_{out}, first-order dissipation rate constant for SV, HR, and TPR; LTDE_{SV} and LTDE_{HR}, percentage of increased baseline SV and HR caused by the time-dependent effect; PP, pulse pressure; RSE, relative standard error; SL_{HR} and SL_{SV}, slope of remifentanyl effect on HR and SV; SV, stroke volume; TPR, total peripheral resistance; γ , Hill coefficient for TPR sigmoid; ρ , correlation coefficient; σ RUV, residual unexplained variability.

Parameter	Estimate (RSE %)	95% Confidence interval	
		Lower	Upper
k _{out} (min ⁻¹)	0.072 (2.8)	0.068	0.076
Base _{SV} (ml)	82.2 (0.7)	81.3	83.3
Base _{HR} (beats min ⁻¹)	56 (0.9)	55	57
Base _{TPR} (mm Hg ml ⁻¹ min ⁻¹)	0.016 (2.4)	0.016	0.017
FB	0.66 (1.7)	0.64	0.68
HR _{SV}	0.312 FIX		
k (min ⁻¹)	0.067 (4.3)	0.061	0.072
LTDE _{SV} (%)	0.090 (4.7)	0.082	0.098
LTDE _{HR} (%)	0.12 (5.2)	0.11	0.13
EC _{50PROP_TPR} (µg ml ⁻¹)	3.21 (2.8)	3.05	3.38
E _{max_PROP_TPR} (%)	-0.78 (1.6)	-0.80	-0.75
Y _{PROP}	1.83 (3.9)	1.69	1.97
EC _{50PROP_SV} (µg ml ⁻¹)	0.44 (2.9)	0.42	0.47
E _{max_PROP_SV} (%)	-0.15 (3.5)	-0.16	-0.14
AGE_E _{max_SV}	0.033 (3.5)	0.031	0.036
EC _{50REMI_TPR} (ng ml ⁻¹)	4.59 (1.7)	4.44	4.76
E _{max_REMI_TPR} (%)	-1 FIX		
SL _{REMI_HR} (ng ml ⁻¹)	0.033 (5.9)	0.029	0.036
SL _{REMI_SV} (ng ml ⁻¹)	0.058 (7.0)	0.051	0.066
INT _{HR} (ng ml ⁻¹)	-0.12 (3.3)	-0.13	-0.11
EC _{50INT_HR} (µg ml ⁻¹)	0.20 (2.9)	0.19	0.21
INT _{TPR} (%)	100.00 (2.3)	95.87	104.51
INT _{SV} (ng ml ⁻¹)	-0.21 (3.3)	-0.23	-0.20
Parameter	BSV%* (RSE %)	95% Confidence interval	
		Lower	Upper
BSV_Base _{SV}	18.3 (7.6); ρ Base _{TPR} -0.58 (7.1)	16.98	19.60
BSV_Base _{TPR}	23.3 (4.1); ρ Base _{HR} -0.65 (8.3)	22.47	24.35
BSV_Base _{HR}	15.67 (7.0)	14.68	16.83
BSV_C _{50PROP_TPR}	74.34 (3.9)	70.50	77.56
BSV_E _{max_REMI_TPR}	75.30 (3.3)	72.07	78.26
BSV_SL _{REMI_HR}	6.18 (12.1); ρ SL _{REMI_SV} 0.57 (13.7)	5.40	6.87
BSV_SL _{REMI_SV}	9.34 (8.9)	8.60	10.20
σ RUV _{Proportional_MAP} (%)	11.04 (1.5)	10.88	11.19
σ RUV _{Proportional_HR} (%)	10.42 (1.5)	10.27	10.57
σ RUV _{Proportional_PP} (%)	17.12 (1.6)	16.88	17.38

Nieuwenhuijs and colleagues,⁹ which predicts that MAP will decrease by 10.6% from baseline (at remifentanyl 1 ng ml⁻¹ and propofol 1 µg ml⁻¹), and HR will decrease by 16.3%. Our model predicts a similar decrease in MAP (11.7%) but a less pronounced effect on HR (2.7%). This discrepancy in predicted HR might partially be explained by the homogenous population in their study, which had a limited range of covariates (healthy males aged 19–25 yr) and prevents reliable evaluation of covariate effects on haemodynamic variables. Furthermore, the dose ranges in their study were relatively low (propofol 0–2.6 µg ml⁻¹; remifentanyl 0–2.0 ng ml⁻¹) compared with our study. Another reason could be that the baroreflex feedback mechanism, which accounts for the increased HR caused by hypotension, was not considered in their study. Therefore, the clinical utility of their study might be limited in terms of its ability to describe mechanistically

the interaction between remifentanyl and propofol on haemodynamics.

We performed a simulation based on the dosing regimen used by Turgut and colleagues³³ to evaluate the potential utility of the interaction model. After induction and maintenance of anaesthesia with propofol and remifentanyl, the mean MAP decreased from 95 to 80 mm Hg in their study, which is in line with predictions from our model with a 95% prediction interval for baseline MAP of 73–117 mm Hg and a MAP during maintenance of anaesthesia between 44 and 84 mm Hg. Their observed changes in HR are also within the 95% prediction intervals from our interaction model.

Our simulations are also in general agreement with observations by Meijer and colleagues,³⁴ who found that 43% of patients experienced a MAP <60 mm Hg, which was 52.5% in our simulations according to their dosing regimen. Similarly,

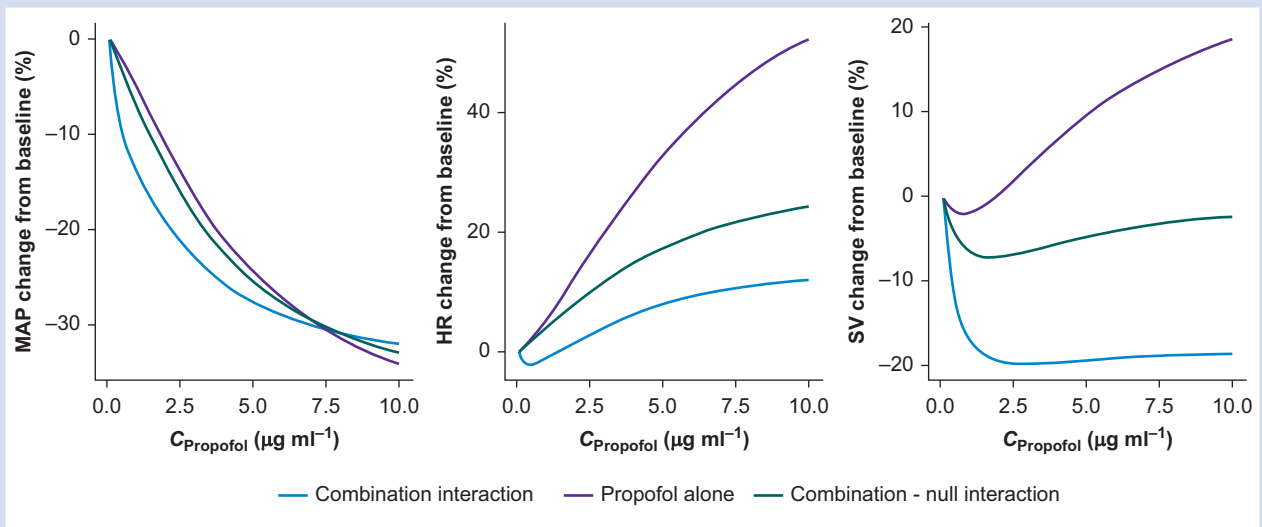


Fig 2. Predicted concentration–effect relationship (change from baseline) of MAP (left), HR (middle), and stroke volume (right) in a 35-yr-old individual for propofol alone (purple) and propofol combined with remifentanil 2 ng ml^{-1} predicted by the combination-null interaction model (green) or the combination interaction model (blue).

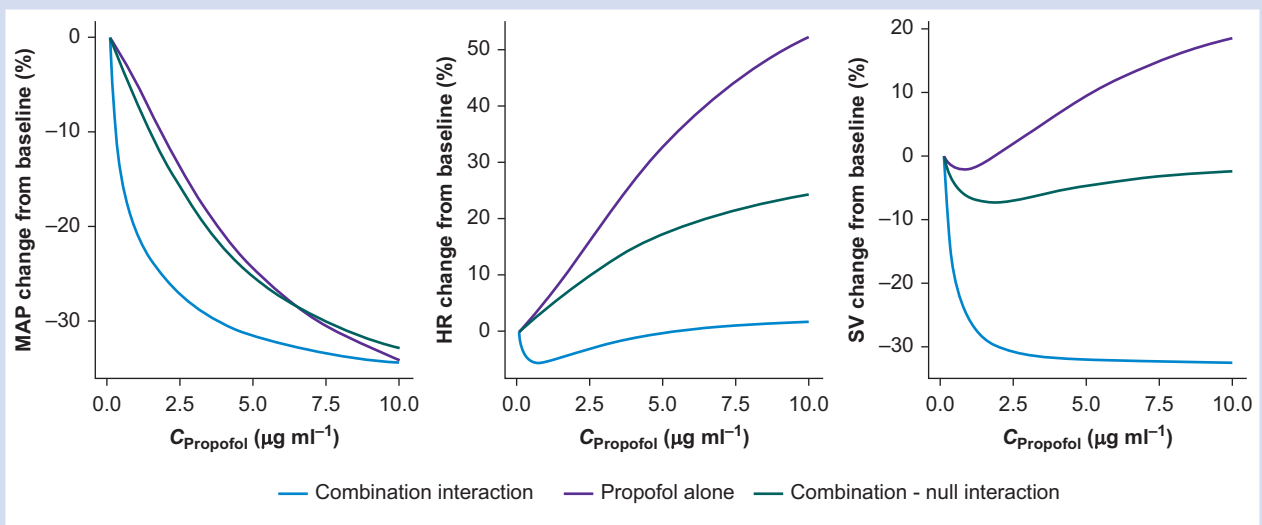


Fig 3. Predicted concentration–effect relationship (change from baseline) of MAP (left), HR (middle), and stroke volume (right) in a 35-yr-old individual for propofol alone (purple) and propofol combined with remifentanil 4 ng ml^{-1} predicted by the combination-null interaction model (green) or the combination interaction model (blue).

Lysakowski and colleagues³⁵ found that HR did not change significantly at a propofol target concentration of $0\text{--}4 \mu\text{g ml}^{-1}$ combined with remifentanil 6 ng ml^{-1} , which is comparable with our simulations. Our mechanism-based haemodynamic model can therefore potentially be used in clinical practice to predict how haemodynamic variables are influenced by propofol, remifentanil, and the combination.

To further support the clinical utility of the mechanism-based haemodynamic model, simulations were performed to

understand the influence of titrating remifentanil on haemodynamics at a stable target concentration of propofol. We found that MAP changed along with the change in remifentanil concentration; however, the most significant change was caused by induction (Supplementary Fig 5–1).

Simulations according to FDA drug label dosing^{25,26} indicated that the interaction model was able to predict the median change in haemodynamic variables and the variability between individuals. The BSV for MAP, HR, and SV could

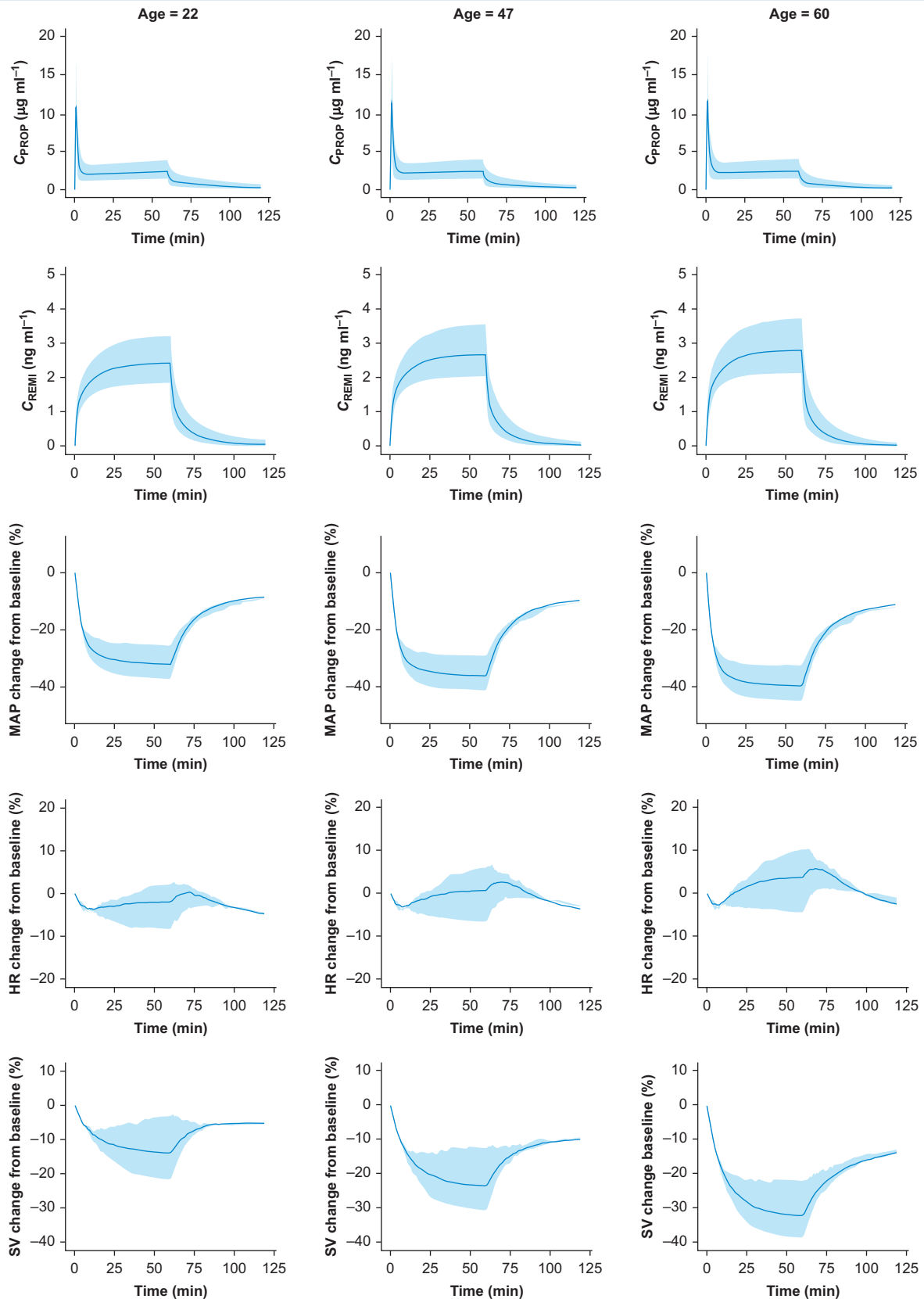


Fig 4. Predicted changes in propofol and remifentanyl plasma concentrations and the relative changes in MAP, HR, and SV baselines during propofol combined with remifentanyl infusion according to the US Food and Drug Administration drug label dosing for different ages. C_{PROP} , plasma concentration of propofol; C_{REMI} , plasma concentration of remifentanyl; SV, stroke volume.

partially be explained by age. The propofol-induced decrease in SV was greater in older individuals, which caused a more pronounced decrease in MAP in the simulation (Fig. 4). This age effect is in agreement with the work by Südfeld and colleagues,³⁶ who showed that the risk for developing hypotension during general anaesthesia increases with age. Thus, to prevent severe haemodynamic side-effects, doses of general anaesthetics should be lower in older patients, which is in line with dosing recommendation in FDA propofol drug label.²⁵ Baseline measurements before surgery can potentially be used to enhance predictions of the model.

There are some limitations to this study. First, data from healthy subjects were used in the development of the mechanistic haemodynamic model of remifentanyl and the interaction model. The ability to identify patient-specific covariates (concomitant medication, comorbidity status, etc.) reliably was therefore limited because of this homogenous population. Use of vasoactive medications, which are often used during induction of general anaesthesia, was not implemented in our model.³⁷ Therefore, the mechanism-based model should be restricted to conditions without vasoactive medication. Second, invasive BP was measured in the remifentanyl-alone group, and noninvasive BP was measured in the propofol and combination groups. There is evidence that noninvasive MAP is in good agreement with invasive MAP.³⁸ However, for critically ill patients, noninvasive BP might not correlate with invasive arterial pressure measurements.³⁹ Based on our data, we could not detect any differences, however. Third, our goal was to inform anaesthesiologists of expected post-induction haemodynamic alterations, in particular post-induction hypotension. Our model was based on data from healthy volunteers and therefore lacks information on the impact of surgical factors. Drug-induced haemodynamic alterations frequently occur during induction of anaesthesia and when surgical stimuli are typically absent.⁴⁰ Nevertheless, the absence of information in the model on the effects of surgical stimulation limits the applicability of the model in these situations. Finally, the influence of typical patient-level confounders (anti-hypertensive medication, vasoactive drugs, frailty, etc.) on the model predictions has not been evaluated. Before clinical use of the model, the predictive performance of the model and the generalisability across patient groups should be prospectively validated.

In conclusion, a mechanism-based haemodynamic model was developed that quantifies the single-drug effects of propofol, remifentanyl, and their combined administration in healthy volunteers. The effects of propofol and remifentanyl cannot be described using the combination-null interaction model, as we identified an antagonistic interaction on HR, a synergistic interaction on stroke volume, and a mixed synergistic antagonistic interaction on mean arterial pressure that depends on the propofol concentration.

Authors' contributions

Study design: MMRFS, PJC

Data analysis: HS, JVK, DJE, PJC

Writing of first draft of paper: HS

Revision of manuscript: JVK, DJE, MMRFS, PJC

Declarations of interest

The research group/department of MMRFS received (over the past 3 yr) research grants and consultancy fees from The

Medicines Company (Parsippany, NJ, USA), Masimo (Irvine, CA, USA), Becton Dickinson (Eysins, Switzerland), Fresenius (Bad Homburg, Germany), Dräger (Lübeck, Germany), Paion (Aachen, Germany), and Medtronic (Dublin, Ireland). He receives royalties on intellectual property from Demed Medical (Temse, Belgium) and Ghent University (Ghent, Belgium). He is an editorial board member and director for the *British Journal of Anaesthesia* and an associate editor for *Anesthesiology*. The other authors declare no competing interests.

Funding

Departmental funding; Masimo; China Scholarship Council to HS (201806010414).

Appendix A. Supplementary data

Supplementary data to this article can be found online at <https://doi.org/10.1016/j.bja.2023.04.043>.

References

1. Noseir RK, Ficke DJ, Kundu A, Arain SR, Ebert TJ. Sympathetic and vascular consequences from remifentanyl in humans. *Anesth Analg* 2003; **96**: 1645–50
2. Sahinovic MM, Struys M, Absalom AR. Clinical pharmacokinetics and pharmacodynamics of propofol. *Clin Pharmacokinet* 2018; **57**: 1539–58
3. Elliott P, O'Hare R, Bill KM, Phillips AS, Gibson FM, Mirakhur RK. Severe cardiovascular depression with remifentanyl. *Anesth Analg* 2000; **91**: 58–61
4. Sneyd JR, Absalom AR, Barends CRM, Jones JB. Hypotension during propofol sedation for colonoscopy: a retrospective exploratory analysis and meta-analysis. *Br J Anaesth* 2022; **128**: 610–22
5. Sessler DI, Sigl JC, Kelley SD, et al. Hospital stay and mortality are increased in patients having a “triple low” of low blood pressure, low bispectral index, and low minimum alveolar concentration of volatile anesthesia. *Anesthesiology* 2012; **116**: 1195–203
6. Soleimani A, Heidari N, Habibi MR, et al. Comparing hemodynamic responses to diazepam, propofol and etomidate during anesthesia induction in patients with left ventricular dysfunction undergoing coronary artery bypass graft surgery: a double-blind, randomized clinical trial. *Med Arch* 2017; **71**: 198–203
7. Su H, Eleveld DJ, Struys M, Colin PJ. Mechanism-based pharmacodynamic model for propofol haemodynamic effects in healthy volunteers. *Br J Anaesth* 2022; **128**: 806–16
8. Standing JF, Hammer GB, Sam WJ, Drover DR. Pharmacokinetic–pharmacodynamic modeling of the hypotensive effect of remifentanyl in infants undergoing cranioplasty. *Pediatr Anesth* 2010; **20**: 7–18
9. Nieuwenhuijs DJF, Olofsen E, Raymonda R, et al. Response surface modeling of remifentanyl–propofol interaction on cardiorespiratory control and bispectral index. *Anesthesiology* 2003; **98**: 312–22
10. Weerink MAS, Barends CRM, Muskiet ERR, et al. Pharmacodynamic interaction of remifentanyl and dexmedetomidine on depth of sedation and tolerance of laryngoscopy. *Anesthesiology* 2019; **131**: 1004–17
11. Kuizenga MH, Colin PJ, Reyntjens K, et al. Test of neural inertia in humans during general anaesthesia. *Br J Anaesth* 2018; **120**: 525–36

12. Eleveld DJ, Proost JH, Vereecke H, et al. An allometric model of remifentanyl pharmacokinetics and pharmacodynamics. *Anesthesiology* 2017; **126**: 1005–18
13. Schnider TW, Minto CF, Gambus PL, et al. The influence of method of administration and covariates on the pharmacokinetics of propofol in adult volunteers. *Anesthesiology* 1998; **88**: 1170–82
14. Schnider TW, Minto CF, Shafer SL, et al. The influence of age on propofol pharmacodynamics. *Anesthesiology* 1999; **90**: 1502–16
15. Minto CF, Schnider TW, Egan TD, et al. Influence of age and gender on the pharmacokinetics and pharmacodynamics of remifentanyl. I. Model development. *Anesthesiology* 1997; **86**: 10–23
16. Minto CF, Schnider TW, Shafer SL. Pharmacokinetics and pharmacodynamics of remifentanyl. II. Model application. *Anesthesiology* 1997; **86**: 24–33
17. Zhang L, Beal SL, Sheiner LB. Simultaneous vs. sequential analysis for population PK/PD data I: best-case performance. *J Pharmacokinetic Pharmacodyn* 2003; **30**: 387–404
18. Eleveld DJ, Colin P, Absalom AR, Struys M. Pharmacokinetic–pharmacodynamic model for propofol for broad application in anaesthesia and sedation. *Br J Anaesth* 2018; **120**: 942–59
19. Wicha SG, Chen C, Clewe O, Simonsson USH. A general pharmacodynamic interaction model identifies perpetrators and victims in drug interactions. *Nat Commun* 2017; **8**: 2129
20. Dosne AG, Bergstrand M, Karlsson MO. An automated sampling importance resampling procedure for estimating parameter uncertainty. *J Pharmacokinetic Pharmacodyn* 2017; **44**: 509–20
21. Bergstrand M, Hooker AC, Wallin JE, Karlsson MO. Prediction-corrected visual predictive checks for diagnosing nonlinear mixed-effects models. *AAPS J* 2011; **13**: 143–51
22. Lindbom L, Ribbing J, Jonsson EN. Perl-speaks-NONMEM (PsN)—a Perl module for NONMEM related programming. *Comput Methods Programs Biomed* 2004; **75**: 85–94
23. Keizer RJ, van Benten M, Beijnen JH, Schellens JH, Huitema AD, Piraña and PCluster: a modeling environment and cluster infrastructure for NONMEM. *Comput Methods Programs Biomed* 2011; **101**: 72–9
24. R Core Team. R: A language and environment for statistical computing. Vienna, Austria: R Foundation for Statistical Computing; 2021. URL, <https://www.R-project.org/>. 31-03-2021
25. US Food and Drug Administration. DIPRIVAN® (propofol) injectable emulsion. USP; 2017. Available from https://www.accessdata.fda.gov/drugsatfda_docs/label/2017/019627s066lbl.pdf
26. US Food and Drug Administration. ULTIVA: remifentanyl hydrochloride 2016. Available from https://www.accessdata.fda.gov/drugsatfda_docs/label/2016/020630s016lbl.pdf.
27. Snelder N, Ploeger BA, Luttringer O, et al. Drug effects on the CVS in conscious rats: separating cardiac output into heart rate and stroke volume using PKPD modelling. *Br J Pharmacol* 2014; **171**: 5076–92
28. Fu Y, Taghvafard H, Said MM, et al. A novel cardiovascular systems model to quantify drugs effects on the inter-relationship between contractility and other hemodynamic variables. *CPT Pharmacometrics Syst Pharmacol* 2022; **11**: 640–52
29. Komatsu R, Turan AM, Orhan-Sungur M, McGuire J, Radke OC, Apfel CC. Remifentanyl for general anaesthesia: a systematic review. *Anaesthesia* 2007; **62**: 1266–80
30. Heijmans JH, Maessen JG, Roekaerts PM. Remifentanyl provides better protection against noxious stimuli during cardiac surgery than alfentanil. *Eur J Anaesthesiol* 2004; **21**: 612–8
31. Mortensen CR, Larsen B, Petersen JA, et al. Remifentanyl vs. alfentanil infusion in non-paralysed patients: a randomized, double-blind study. *Eur J Anaesthesiol* 2004; **21**: 787–92
32. Bouillon T, Bruhn J, Radu-Radulescu L, Bertaccini E, Park S, Shafer S. Non-steady state analysis of the pharmacokinetic interaction between propofol and remifentanyl. *Anesthesiology* 2002; **97**: 1350–62
33. Turgut N, Turkmen A, Ali A, Altan A. Remifentanyl–propofol vs dexmedetomidine–propofol–anaesthesia for supratentorial craniotomy. *Middle East J Anaesthesiol* 2009; **20**: 63–70
34. Meijer FS, Martini CH, Broens S, et al. Nociception-guided versus standard care during remifentanyl–propofol anaesthesia: a randomized controlled trial. *Anesthesiology* 2019; **130**: 745–55
35. Lysakowski C, Dumont L, Pellegrini M, Clergue F, Tassonyi E. Effects of fentanyl, alfentanil, remifentanyl and sufentanil on loss of consciousness and bispectral index during propofol induction of anaesthesia. *Br J Anaesth* 2001; **86**: 523–7
36. Südfeld S, Brechnitz S, Wagner JY, et al. Post-induction hypotension and early intraoperative hypotension associated with general anaesthesia. *Br J Anaesth* 2017; **119**: 57–64
37. Poterman M, Vos JJ, Vereecke HEM, et al. Differential effects of phenylephrine and norepinephrine on peripheral tissue oxygenation during general anaesthesia: a randomised controlled trial. *Eur J Anaesthesiol* 2015; **32**: 571–80
38. Seidlerová J, Tümová P, Rokyta R, Hromadka M. Factors influencing the accuracy of non-invasive blood pressure measurements in patients admitted for cardiogenic shock. *BMC Cardiovasc Disord* 2019; **19**: 150
39. Riley LE, Chen GJ, Latham HE. Comparison of noninvasive blood pressure monitoring with invasive arterial pressure monitoring in medical ICU patients with septic shock. *Blood Press Monit* 2017; **22**: 202–7
40. Löffel LM, Bachmann KF, Furrer MA, Wuethrich PY. Impact of intraoperative hypotension on early post-operative acute kidney injury in cystectomy patients—a retrospective cohort analysis. *J Clin Anesth* 2020; **66**, 109906